AMERICAN
METEOROLOGICAL
SOCIETY

Journal of Hydrometeorology

EARLY ONLINE RELEASE

The DOI for this manuscript is doi: 10.1175/JHM-D-13-063.1

The final published version of this manuscript will replace the preliminary version at the above DOI once it is available.

If you would like to cite this EOR in a separate work, please use the following full citation:

Kala, J., M. Decker, J. Exbrayat, A. Pitman, C. Carouge, J. Evans, G. Abramowitz, and D. Mocko, 2013: Influence of leaf area index prescriptions on simulations of heat, moisture, and carbon fluxes. J. Hydrometeor. doi:10.1175/JHM-D-13-063.1, in press.

Influence of leaf area index prescriptions on simulations of heat, moisture, and carbon fluxes

Jatin Kala, * Mark Decker, Jean-François Exbrayat, Andy J. Pitman, Claire Carouge, Jason P. Evans, Gab Abramowitz

ARC Centre of Excellence for Climate Systems Science and Climate Change Research Centre, UNSW, Australia

David Mocko

SAIC at NASA Goddard Space Flight Centre, NASA, Greenbelt, MD, USA

*Corresponding author address: Jatin Kala, Australian Research Council Centre of Excellence for Climate Systems Science and Climate Change Research Centre, University of New South Wales, Sydney, NSW, 2052, Australia.

E-mail: J.Kala@unsw.edu.au or Jatin.Kala.JK@gmail.com

ABSTRACT

Leaf-area index (LAI), the total one-sided surface area of leaf per ground surface area, is a key component of land surface models. We investigate the influence of differing, plausible LAI prescriptions on heat, moisture, and carbon fluxes simulated by the Community Atmosphere Biosphere Land Exchange (CABLEv1.4b) model over the Australian continent. A 15-member ensemble monthly LAI data-set is generated using the MODIS LAI product and gridded observations of temperature and precipitation. Offline simulations lasting 29 years (1980-2008) are carried out at 25 km resolution with the composite monthly means from the MODIS LAI product (control simulation) and compared with simulations using each of the 15-member ensemble monthly-varying LAI data-sets generated. The imposed changes in LAI did not strongly influence the sensible and latent fluxes but the carbon fluxes were more strongly affected. Croplands showed the largest sensitivity in gross primary production with differences ranging from -90 to 60 %. PFTs with high absolute LAI and low inter-annual variability, such as evergreen broadleaf trees, showed the least response to the different LAI prescriptions, whilst those with lower absolute LAI and higher inter-annual variability, such as croplands, were more sensitive. We show that reliance on a single LAI prescription may not accurately reflect the uncertainty in the simulation of the terrestrial carbon fluxes, especially for PFTs with high inter-annual variability. Our study highlights that the accurate representation of LAI in land surface models is key to the simulation of the terrestrial carbon cycle. Hence this will become critical in quantifying the uncertainty in future changes in primary production.

1. Introduction

Land Surface Models (LSMs) describe the exchange of heat, moisture, and carbon between the land surface and the atmosphere. There are a wide variety of LSMs used in both regional and global climate models, and they can vary considerably in complexity (Pitman 2003). One key aspect which differentiates LSMs is whether they include phenology, and if dynamic, whether it is prescribed or simulated. In most LSMs, phenology is represented by the leaf area index (LAI), the total one-sided surface area of leaf per ground surface area.

LAI is critical in any LSM since it affects the albedo of the terrestrial surface, and hence, the amount of net radiation available to drive sensible and latent heat. LAI also affects the partitioning of net radiation between sensible and latent heat fluxes (Verstraete and Dickinson 1986) because it controls the surface area of vegetation in direct contact with the atmosphere and affects the efficiency by which water can be transferred from within the vegetation to the atmosphere. Similarly, LAI affects the terrestrial carbon balance since it affects the photosynthesis and net primary productivity of a canopy. Finally, LAI influences rainfall interception and thereby affects the partitioning of rainfall between evaporation, throughfall, and runoff.

The implementation of LAI in LSMs within regional and global climate models varies widely. At one end of the spectrum, some LSMs are coupled to dynamic vegetation models (e.g., Bonan et al. 2003), whereby LAI is a prognostic variable and responds to surface climate variations. However, climate biases from the regional and global atmospheric models make the realistic simulation of LAI difficult (Liu et al. 2008). As a consequence, most LSMs do not include dynamic vegetation and instead prescribe LAI.

LAI can be prescribed according to plant functional types (PFTs) from look-up tables. These values are usually based on field observations and either held constant in time or allowed to vary seasonally. This method does not allow for inter-annual variability or variations within PFTs; the same PFTs at different latitudes use the same LAI. Since this is not realistic, several studies have investigated the use of satellite derived LAI and shown

improvements in the simulation of surface climatology (e.g., Pielke et al. 1997; Buermann et al. 2001). The main impediment to the use of satellite derived LAI is the limited temporal availability of these data. There is also an inherent assumption of stationarity for future climate simulations; the assumption that the present spatial and seasonal variations in LAI are representative of the future, even though they are clearly climate-dependant.

Since LAI interacts with radiation, water balance and carbon balance it is a key parameter connecting the core components of climate and ecological modeling (Parton et al. 1996). One of the key characteristics of LAI is how it varies spatially (Bonan et al. 1993) and temporally. While LAI affects the interactions between the atmosphere at a point or grid scale (Bonan et al. 1993) this scales up to continental scales (Pitman et al. 1999) in uncoupled simulations. There is additional evidence that LAI affects the atmosphere at larger scales (Chase et al. 1996). Most recently, van den Hurk et al. (2003) demonstrated that using remotely sensed LAI in a weather forecasting system affected the surface evaporation when evaporation formed a large term in the surface energy balance. They concluded that improved estimates of LAI could be an important method for improving model estimates of evaporation.

The relationship between LAI and the terrestrial carbon balance is well documented from observational studies. Barr et al. (2004) investigated the influence of LAI on net ecosystem production in a deciduous forest in Canada and found a tight coupling between the annual maximum LAI and production. Saigusa et al. (2008) used data from flux-towers and found that temperate deciduous forests showed the greatest positive net ecosystem production after leaf expansion (higher LAI) in early summer. Duursma et al. (2009) used measurements from coniferous stands in Europe and found that LAI was a significant influence on gross primary production (GPP). Finally, Keith et al. (2012) used measurements at a single flux-tower site in Australia and focused on the carbon budget during drought years. They found that reductions in LAI due to insect attacks, in addition to drought stresses, contributed to a 26% reduction in GPP and 9% reduction in ecosystem respiration as compared to years with drought stresses alone.

Some modelling studies have investigated the influences of vegetation parameters on the simulation of the terrestrial carbon fluxes and season length (e.g., White and Nemani 2003; Piao et al. 2007), but few explicitly focus on the influence of LAI versus meteorological forcing. This was recently investigated by Puma et al. (2013) in an offline LSM at four North American sites. They found that variations in LAI had a dominant control on GPP, a smaller but comparable effect on transpiration, a weak influence on total evapotranspiration, and a negligible impact on runoff. Additionally, they found that the effect of LAI on GPP is greater in energy-limited regimes as compared to moisture-limited regimes, except when vegetation exhibits little inter-annual variations in LAI. Hence, they conclude that an accurate representation of LAI inter-annual variability in LSMs is critical to accurately simulate GPP.

Overall, it is clear that the way a LSM treats LAI is central to accurately simulating the heat, moisture, and carbon fluxes at the land surface. This paper focuses on the Community Atmosphere Biosphere Land Exchange Model (CABLE) (Wang et al. 2011). CABLE does not include a dynamic vegetation model by default, and hence the spatial and temporal variation of LAI are prescribed (prognostic LAI is implemented in later versions but not currently widely used). While several studies have used CABLE to answer wide-ranging research questions (e.g., Abramowitz and Gupta 2008; Cruz et al. 2010; Zhang et al. 2011b; Pitman et al. 2011; Wang et al. 2012; Exbrayat et al. 2012), only few studies have examined the influence of LAI on heat, moisture and carbon fluxes in CABLE.

Zhang et al. (2013) ran global offline simulations with CABLE and conducted a sensitivity analysis by varying several vegetation and soil parameters, including LAI, by $\pm$ 50, 30, and 20 % of the default values. Comparison of their simulations with other models (Rodell et al. 2004; Dirmeyer et al. 2006; Jung et al. 2009) showed that the influence of LAI was most noticeable in the middle and high latitudes of the northern hemisphere where broadleaf forests are the dominant PFT. However, Zhang et al. (2013) also point out that their imposed LAI perturbation do not necessarily reflect realistic uncertainties in estimates of LAI, and

additionally, only focussed on evapotranspiration and run-off.

Lu et al. (2013) conducted an extensive parameter sensitivity analysis of CABLE over a single year at the global scale. They found that the at the global scale, the most important parameter affecting GPP is the maximum carboxylation rate, followed by LAI. When analysing each PFT separately, they also found LAI to be the second most important parameter influencing GPP, except for evergreen broadleaf forests, whereby the initial slope of the response curve of potential electron was the second most important factor, followed by LAI. They carried out a similar analysis for latent heat, and found LAI to be the third most important factor globally, but results varied for each PFT. Namely, LAI was the most important for deciduous needleleaf trees, second most important for evergreen needleleaf trees, third most important for evergreen broadleaf trees, deciduous broadleaf trees, and deciduous needleleaf trees, fourth most important for crops, and fifth most important for shrublands.

Whilst the work of Zhang et al. (2013) and Lu et al. (2013) provide valuable insight into the sensitivity of CABLE to LAI, and it's importance relative to other model parameters, the influence of realistic inter-annual variations in LAI on the surface energy and carbon balance remains un-known. This study provides a method of generating LAI ensembles, based on the MODIS LAI and the observed climatology, to address this knowledge gap. The next section describes the model set-up and the generation of the LAI ensemble. This is followed by an analysis of the influence of different monthly-varying LAI prescriptions on CABLE simulated surface energy and carbon fluxes.

2. Methods

a. Model Description

CABLE is a LSM designed to simulate fluxes of energy, water and carbon at the land surface and can be run as an offline-model with prescribed meteorology (e.g., Wang et al. 2011) or fully coupled to an atmospheric model within a global or regional climate model

(e.g., Mao et al. 2011). CABLE is a key part of the Australian Community Climate Earth System Simulator (ACCESS, see `http://www.accessimulator.org.au`), a fully coupled earth system science model, currently being used as part of the fifth assessment report of the International Panel on Climate Change. The version used in this study is CABLEv1.4b.

In CABLEv1.4b, the one-layered, two-leaf canopy radiation module of Wang and Leuning (1998) is used for sunlit and shaded leaves and the canopy micro-meteorology module of Raupach (1994) is used for computing surface roughness length, zero-plane displacement height, and aerodynamic resistance. The model also consists of a surface flux module to compute the sensible and latent heat flux from the canopy and soil, the ground heat flux, as well as net photosynthesis. A soil module is used for the transfer of heat and water within the soil and snow, and an ecosystem carbon module based on Dickinson et al. (1998) is used for the terrestrial carbon cycle. A detailed description of each of the modules can be found in Kowalczyk et al. (2006) and Wang et al. (2011).

LAI in CABLE is used to compute the roughness length of vegetation and the standard deviation of vertical velocities, which are used for the formulation of the aerodynamic resistances, and hence influence surface energy balance calculations. It is also used to compute the total flux density of radiation for sunlit and shaded leaves within the plant canopy radiation transfer model. This influences simulations of photosynthesis, stomatal conductance, leaf temperature, and energy and carbon fluxes as CABLE performs separate calculations for sunlit versus shaded leaves (Kowalczyk et al. 2006). Finally, LAI is used in the ecosystem carbon module where it directly influences GPP and autotrophic respiration (AR). Heterotrophic respiration (HR) is not directly driven by LAI, but by soil moisture and temperature.

b. Model set-up

CABLEv1.4b was used within the NASA Land Information System (LIS-6.1) (Kumar et al. 2006, 2008), a flexible software platform designed as a land surface modelling and

hydrological data assimilation system. A grid resolution of 0.25 × 0.25 degrees was utilised, covering continental Australia. The model was forced with the Modern Era Retrospective-analysis for Research and Applications (MERRA) reanalysis (Rienecker et al. 2011) at 3-hourly intervals and integrated from 1980-2008 and initialised from a previous 30-year spin-up. The forcing variables included incoming long-wave and short-wave radiation, air temperature, specific humidity, surface pressure, wind speed and precipitation. The MERRA reanalysis was bias-corrected for precipitation using the Australian Bureau of Meteorology Australian Water Availability gridded precipitation dataset (Jones et al. 2009), following Decker et al. (2012). Monthly ambient carbon-dioxide concentrations were prescribed using measurements from Baring Head, New Zealand (Keeling et al. 2005).

In CABLEv1.4b, the background snow-free and vegetation-free soil albedo has to be prescribed. We used the MODIS derived snow-free background soil albedo data from Houldcroft et al. (2009). Bare soil regions, as defined by the IGBP land-use classification map (used in CABLE), are assigned the mean albedo over the data period (October 2002 to December 2006), whilst partially vegetated pixels are assigned a soil albedo derived from a linear relationship between albedo and the Normalised Difference Vegetation Index (NDVI). A linear regression model is then used to estimate the background soil albedo corresponding to zero green LAI (Houldcroft et al. 2009). The IGBP land-use classification was used, and radiative properties, including the leaf transmittance and reflectance values in the visible, near infra-red, and thermal regions were prescribed for each vegetation type following Avila et al. (2012). These values were obtained by adjusting estimates from Dorman and Sellers (1989) until the simulated albedo from CABLE closely approximated the MODIS observed broadband albedo.

c. Simulations

When running CABLE at a single site, LAI can be prescribed from observations at the site (e.g., Abramowitz and Gupta 2008; Wang et al. 2011; Li et al. 2012). When running

CABLE over a grid domain, LAI values are by default taken from a literature-based estimate for each PFT, and are fixed in time (e.g., Zhang et al. 2011a) or vary seasonally (Avila et al. 2012). For IPCC AR5 global climate simulations, the MODIS LAI product is used in CABLE within the ACCESS global circulation model. Since the aim of this paper is better inform the sensitivity of CABLE to LAI, we use the same MODIS LAI product (Yuan et al. 2011) for our control simulation (1980-2008). This is carried out by prescribing monthly mean climatological LAI at each grid cell, based on monthly averages over the period of availability of the MODIS LAI data (2000-2008).

To investigate the influence of LAI, a 15-member monthly-varying (1980-2008) LAI ensemble was generated using the MODIS LAI and gridded observations of maximum (Tmax) and minimum (Tmin) temperatures and precipitation from the Bureau of Meteorology Australian Water Availability Project (BAWAP) (Jones et al. 2009). The goal of reconstructing the LAI was to explore the model response to reasonable estimates of LAI variability and therefore, an ensemble approach based on simple linear regression between the MODIS LAI and the BAWAP data was used.

The 8-day MODIS LAI was spatially aggregated from its original 0.05 by 0.05 degree grid to the BWAP 0.25 by 0.25 degree grid, by weighting each 0.05 cell by the area, summing the twenty-five 0.05 degree grid cells within each 0.25 cell, and finally normalizing by the total area within the course grid cell. This simple method avoids introducing unnecessary complexities that arise when the LAI is interpolated using subgrid scale plant functional type distributions. The 8-day, 0.25 degree fields where finally averaged to the monthly means by weighting each 8-day period according to the number of days from that time-span that fell within a given month.

The 15-ensemble members were generated by linearly regressing the anomalous (found by removing the mean annual cycle) monthly MODIS LAI against Tmax, Tmin, and precipitation from BAWAP at each 0.25^{o} grid cell. The regressions were performed using data from the period 2000-2008, as this period is coincident with availability of the MODIS LAI.

The regressions were first performed separately for each variable and subsequently using all three variables to isolate the influence of each of Tmax, Tmin, and precipitation. Due to the lag between precipitation and vegetation greenness metrics in Southeastern Australia (Decker et al. 2012) we use a centered 5-point linear regression, although similar results are obtained when only three points are included. The different sets of spatially distributed regression coefficients were calculated by randomly removing 25% of the data from each of the 15 regressions.

Data was withheld as the data training period (2000-2008) occurs during a long-term, large scale drought in Australia. Limiting the temporal data in each of the regressions allows for uncertainty due to the training period selection and creates a larger spread among the final ensemble members. The 15 ensemble estimates of anomalous LAI were created by applying each of these 15 different, spatially explicit regression coefficients for the period 1980-2008. A random Gaussian noise component with the mean and standard deviation given by the mean and standard deviation of the regression errors from each fitting was added during the construction of the LAI estimates. The added noise ensures that the errors associated with the fitting propagates to the final estimates, increases the spread between each of the ensemble members, and is consistent with the assumption that errors in LAI follow a Gaussian distribution (McColl et al. 2011). Finally these estimates of the LAI anomalies (constructed using all three data sources) were added to the mean annual cycle of the MODIS LAI to create the final LAI ensemble members. The spatially averaged ensemble spread of the anomalous LAI, relative to (i.e. divided by) the spatially averaged ensemble mean anomaly was 19.1% for the median, 22.9 % for the mean, 0.1 % for the minimum, and 133.6 % for the maximum. Whilst this range of LAI is smaller as compared to the range of LAI imposed by other studies, it suits the purpose of testing the influence of a climatologically driven LAI ensemble which is the aim of this study.

Figure 1 shows the relationship between the MODIS LAI and the mean of the 15 member ensemble LAI reconstructions using only precipitation (Figure 1a), Tmax (Figure 1b), Tmin

(Figure 1c), and the combination of all three (Figure 1d). The root mean square errors (RMSE) of the single variable regressions are 0.190, 0.194, and 0.200 respectively, while using all three variables results in a slightly better fitting (with an RMSE of 0.188). Figure 1 demonstrates that while precipitation, Tmax, and Tmin, can be used to reconstruct the LAI, the slope of the fittings are less than one (0.982, 0.981, and 0.980, respectively). The combination of the three (Figure 1d) yield a slope of 0.987, which is statistically larger than the slopes of the regressions using a single variable but still less than one. Due to the slightly better agreement with the MODIS observations for the period 2000-2008, the LAI reconstructed using all three variables was used for the model simulations. Overall the mean of the ensemble members reconstructs the LAI variability for the period 2000-2008 with R2 values typically 0.3-0.6, with some individual ensemble members better matching the observed LAI variability over this period.

15 simulations were performed over this period using these monthly-varying LAI reconstructions. We note here that several studies on the influence of LAI on surface climatology use time-varying versus fixed LAI (e.g., van den Hurk et al. 2003) or apply a fixed factor (e.g., double or half LAI, (Parton et al. 1996)). Since it is well established that the seasonal variation of LAI is not negligible (e.g., over croplands), and the use of remotely sensed LAI in LSMs generally improves surface climatology (Pielke et al. 1997; Buermann et al. 2001), we focus here on one of the most widely adopted remotely-sensed LAI products, MODIS, and examine the sensitivity of CABLE to a MODIS-derived monthly varying ensemble LAI product, which is representative of the climatology. In summary, both the control and experiments are run over the same time-period, except that the control simulation has no inter-annual variation in LAI while the ensemble members are designed to reflect the climatology.

d. Data analysis

The heat, moisture, and carbon fluxes were analysed separately for each dominant PFT, defined as PFTs with coverage greater than 1% of land points as shown in Figure 2. This was to avoid compensating effects between PFTs, as these have distinct seasonal signals as well as absolute magnitudes. For example, croplands, being a human-managed PFT, have higher seasonal variability than native vegetation. Additionally, the dense forested areas (evergreen broadleaf trees), have the highest absolute LAI, while most of inland Australia is sparsely vegetated with open shrublands with lower absolute LAI. Since the imposed changes in LAI are on the monthly time-scale, we compute monthly means and standard deviations of the fluxes and plot time series of the difference between the control and ensemble mean, with the standard deviation used to provide a measure of spread. Since the variations in the imposed LAI vary with time (monthly) and reflect the inter-annual variability in climatology inherent in the BAWAP gridded precipitation and temperature data-set, we perform a time-series rather than seasonal analysis (e.g., mean summer fluxes over the whole period). Additionally, we compute zero-lag cross-correlations between LAI and the fluxes to better quantify the response to changes in LAI.

3. Results

Figure 3 shows a monthly time-series of (a) the absolute (control-ensemble mean), and (b), percentage difference ((absolute difference/control)$\times$100) in LAI, heat, moisture, and carbon fluxes for open shrublands between 1980-2008. The zero-lag cross correlations with LAI are summarised in Table 1. The difference in LAI for open shrublands varies approximately between -0.2 to 0.1, which represents a percentage change of -90 to 30 %. As expected, increases in LAI lead to a increase in vegetation transpiration (EV) and an decrease in soil evaporation (ES) as shown by the strong positive cross-correlation between LAI and EV and negative correlation with ES (Table 1). Although the absolute changes in EV are smaller

than ES, when expressed as a percentage change, they are larger by a factor of $\sim$ 2-3. This is expected as the amount of leaf respiration is a direct function of LAI, whereas LAI only acts to partially inhibit soil evaporation.

The effects of LAI on the absolute changes in mean monthly sensible (Qh) and latent (Qle) heat fluxes are small ($< 1\,\mathrm{W\,m^{-2}}$), with percentage changes between -4 to 6 % only, and the correlations with LAI are lower as compared to EV and ES. These small changes in Qh and Qle corresponded with equally small changes in net radiation and surface albedo (not shown). Overall surface albedo in CABLE is a function of the vegetation albedo, background snow-free soil albedo, and snow albedo. The area covered by open shrublands is not densely vegetated, and hence it is the background soil albedo which largely determines the overall surface albedo. Thus, the relatively small perturbation in LAI imposed did not alter the overall surface albedo to a large extent and hence, the partitioning between Qh and Qle was not generally affected.

The changes in the terrestrial carbon fluxes, on the other hand, showed a much stronger response to LAI. A decrease in LAI led to a decrease in autotrophic respiration (AR), and increase in heterotrophic respiration (HR), with strong positive cross-correlation between LAI and AR and weaker negative correlation with HR (Table 1).When expressed as a percentage change, the differences in AR were up to 3-4 times larger than HR. This was expected, since HR is driven by below-canopy and soil processes, whilst AR is a direct function of LAI. Similarly, GPP was strongly positively correlated with LAI (we note that by convention in CABLE, downwards fluxes (i.e., GPP) are negative, but shown as positive here to remain consistent with the literature), as it is also a direct function of LAI, with percentage differences between -40 to 20 % (the same order of magnitude as the percentage change in LAI).

For croplands (Figure 4), the absolute change in LAI varies between -0.6 and 0.6, corresponding to a percentage change of approximately -160 to 40 %. This is larger when compared to open shrublands and all the other PFTs. Croplands, being a human-managed

PFT, have the highest seasonal and inter-annual variation in LAI ($\sim$ 0.3-1.8) as compared to open shrublands ($\sim$ 0.3-0.5) and the other PFTs, and hence the strongest response to monthly changes in precipitation, Tmax, and Tmin, which were used to generate the ensemble. The absolute changes in the heat and evaporative fluxes are an order of magnitude higher as compared to open shrublands (Figure 3), and the corresponding percentage changes are about double. Although the absolute changes in Qh and Qle are larger as compared to open shrublands, this change on a monthly time-scale is relatively small (the large percentage changes in Qh of up to 600 % still represent a small absolute change). The small absolute LAI of croplands is such that even large percentage changes did not change the surface albedo to a large enough extent to significantly alter net radiation. The absolute changes in AR, HR, and GPP are also an order of magnitude larger as compared to open shrublands, and the percentage changes are comparable to the imposed change in LAI.

The changes for the other PFTs (woody savannas, savannas, and grasslands) showed similar trends (not shown), most noticeable in the carbon, rather than the turbulent heat fluxes. Evergreen broadleaf trees (Figure 5) had the smallest percentage change in LAI, since they have the largest absolute LAI values, and low inter-annual variability ($\sim$ 2.8-3.4). Hence, this PFT had the smallest response in the carbon fluxes (-4 to 6 %), with lower cross-corrrelations to LAI as compared to the other PFTs (Table 1). Evergreen broadleaf trees also showed a small positive correlation to HR of 0.46 (Table 1), whilst all other PFTs had a negative correlation, showing that a dense canopy can enhance HR. Another noticeable result for Evergreen broadleaf trees was that soil evaporation had a larger response to LAI as compared to vegetation transpiration in both absolute and percentage terms. This was a counter-intuitive result, as dense forested canopies would be expected to have a larger response of vegetation evaporation to LAI as compared to soil evaporation. To further investigate this, we conduced two extra simulations with large perturbations to the control LAI of $\pm$ 50 %.

Figure 6 shows the seasonal difference in LAI imposed between the two experiments

(+50% minus -50%) and the subsequent changes to vegetation and soil evaporation (we show contours rather than time-series as the imposed LAI for these simulations has no inter-annual variability). As expected, a doubling of LAI results in an overall increase in vegetation transpiration and decrease in soil evaporation. However, the decrease in soil evaporation is almost twice as large as in the increase in vegetation transpiration, especially along the east coast where most Evergreen broadleaf trees are found. This is further demonstrated in Figure 7, showing the fraction of vegetation transpiration as a function of evapotranspiration (vegetation + soil) for both experiments. Over a semi-arid continent, changes in LAI result in a stronger response of soil evaporation as compared to vegetation transpiration.

Whilst there are clear differences in the month-to-month variation of the heat, moisture, and carbon fluxes, increases in one period may be cancelled by a decrease later on. Additionally, we have not considered any spatial patterns in the changes in LAI and carbon fluxes. This is illustrated in Figure 8, showing the gridded cumulative monthly mean difference in LAI on carbon fluxes (cumulative changes in LAI < 5 have been masked out to highlight the largest changes). Clearly, the largest changes in LAI and carbon fluxes are restricted to the southeastern, rather than southwestern croplands (see Figure 2). This is due to the imposed change in LAI being almost twice as high for the southeastern as compared to the southwestern croplands, as illustrated in Figures 9a and 9b respectively. The larger response to LAI in southeast is due to the larger inter-annual variation in precipitation in this region, which was used to generate the LAI ensemble.

4. Discussion

The literature clearly suggests that the prescription of LAI in LSMs has a strong influence on the surface heat, moisture, and carbon fluxes. Hence we conducted a series of experiments to examine the influence of LAI variability in CABLE, as it is a widely used LSM in the Australian climate community and this sensitivity has not been previously tested.

Our results show relatively small impacts on the partitioning of available energy into the sensible and latent heat fluxes. Other studies have found much larger impacts, however, these were confined to regions of much larger changes in LAI compared to the changes imposed in this study. For example, Pitman et al. (1999) found large changes in total evaporative fluxes, but these were confined to regions where the absolute change in LAI was up to 3. Similarly, Bonan et al. (1993) found that LAI had a strong influence on the surface energy balance, but focussed on western US Conifer forests, the LAI of which varies from approximately 5 to 13. The imposed changes in LAI were much smaller in magnitude, but realistic and plausible , i.e., related to the climatology. Even when the LAI was doubled, the magnitude of the change was less than 1 for most of the continent (Fig. 6 (a)). Hence, the relatively small response of the evaporative fluxes is due to a small (but realistic) perturbation in LAI.

The experiments with $\pm$ 50 % of the control LAI showed that doubling LAI resulted in a decrease in soil evaporation, which is twice as large as the increase in vegetation transpiration. This result is consistent with other studies which have shown that over half of the water lost through evapotranspiration over the Australian continent is through soil evaporation and by-passes plants almost entirely (Haverd et al. 2013). Similar results have been found elsewhere. Namely, van den Hurk et al. (2003) showed that in relatively dry (moisture limited) areas, where LAI values are relatively low, changes in LAI cannot result in large changes in surface heat and moisture fluxes as the land surface is already constrained by available soil water. In other words, variations in LAI cause the stronger response where surface evaporation uses a large proportion of the available energy.

van den Hurk et al. (2003) did not allow for changes in LAI to alter the surface albedo, and hence, omitted a feedback important to our results. In our simulations, the variations in LAI imposed resulted in small changes in surface albedo, and subsequently small changes in net radiation. The small change in albedo is due to the relatively small perturbation in LAI imposed and because Australia is sparsely vegetated over large regions. It is therefore the background soil albedo, rather than the vegetation albedo, which has a large influence

on overall surface albedo in these regions.

We found larger impacts on the terrestrial carbon balance, with LAI strongly positively correlated to GPP and AR, and negatively correlated with HR, consistent with both observational (Barr et al. 2004; Saigusa et al. 2008; Duursma et al. 2009; Keith et al. 2012) and modelling (Puma et al. 2013) studies which report a tight coupling between LAI and primary production. This tight coupling is not unexpected as LAI is a key variable in the parameterisation of the carbon cycle. It determines not only the area of leaf that is potentially available to absorb light (and fix carbon via primary production, i.e., GPP), but also the amount of light attenuated and precipitation intercepted by the canopy. This in turn influences soil temperature, moisture, and evaporation, which drive heterotrophic respiration. However, of greater interest is the net ecosystem exchange (NEE) of carbon, i.e., the difference between GPP and the sum of HR and AR. If NEE in negative, then the land surface is a net source of carbon and a sink when positive. In all our simulations, NEE was always positive for both the control and the ensemble mean, and hence, the changes in LAI did not change the land surface to a source of carbon.

The largest impacts were found for croplands, which have the highest inter-annual variability in LAI. The changes were mostly restricted to the southeast, rather than southwest croplands, as the imposed changed in LAI was almost double in the former compared to the latter region. The southeast of Australia experiences higher inter-annual rainfall variability as compared to the southwest due to large-scale teleconnections (Risbey et al. 2009), and this signal was reflected in the LAI ensemble produced, as it is derived using gridded, station based precipitation and temperature data. The least impact was found for evergreen broadleaf trees, which had highest absolute LAI and lowest inter-annual variability. These results are consistent with Guillevic et al. (2002) and Puma et al. (2013), namely, that the impact of LAI variability is less for denser vegetation and moisture limited regions (low evaporative fraction).

Whilst our results are broadly consistent with existing literature, they are constrained

by several caveats inherent of the study design. The model grid domain was restricted to Australia, due to the spatial extent of the BAWAP precipitation and temperature data used for generating the LAI ensemble, as well as bias correcting the forcing data. Hence our results are largely applicable to arid and/or semi-arid regions. Nonetheless, the results presented here should help inform the design of a broad range of future climate simulations whereby LAI is prescribed, especially when the focus is on the terrestrial carbon cycle. Our results are also limited to one particular LSM driven offline with a particular atmospheric forcing. Thus, our results would results would be worth extending via a multi-model evaluation of the sensitivity of LAI in LSMs that simulate the terrestrial carbon cycle. Despite inevitable caveats, our results highlight that the sensitivity testing of LSMs to LAI should be extended to include the terrestrial carbon cycle (rather than just heat and moisture fluxes). Additionally, the sensitivity of crop biomes to LAI highlights a need for the better representation of crop phenology in LSMs. This however remains a difficult challenge as crops, in contrast to other PFTs, are strongly and directly influenced by human intervention.

5. Conclusions

LAI is a critical component of any LSM. In this study, we performed a sensitivity analysis of heat and carbon fluxes to perturbations in LAI using the CABLE LSM over the Australian continent on a monthly time-scale. We showed that whilst the influences of LAI perturbations on the heat and moisture fluxes were low, the impact on the terrestrial carbon balance was large, especially for croplands. Our results are consistent with earlier studies which have shown that PFTs with high inter-annual variability are the most sensitive to LAI perturbations, whilst dense vegetation is less sensitive, especially in moisture limited regimes. A key conclusion is therefore that care should be taken in accurately prescribing LAI, particularly when simulating the carbon cycle. Clearly, assigning fixed LAI to PFTs and/or using climatological means from remote sensing products, will not accurately reflect

the interannual variability of LAI which can have a large impact on the cumulative carbon fluxes.

While our results focus on Australia, they provide several useful conclusions to the broader LSM community. First, using an ensemble of LAI products in simulations can be a very useful and straightforward method in establishing one element of uncertainty and the method used to generate the LAI ensemble here can be adapted to other regions and/or globally. Second, there is a clear need to assess the influence of LAI on the terrestrial carbon cycle at the global scale. To our knowledge, no studies have systematically addressed this issue, and this would provide a means to better quantify the uncertainty in future changes in the global terrestrial carbon cycle. Third, the sensitivities we find to LAI, particularly in respect of terrestrial carbon, points to the urgent need to resolve the parameterization of LAI more systematically in LSMs. Ideally, this is not through better prescriptions of LAI, rather it is via the addition of leaf phenology modules to LSMs. This highlights an important area of development in CABLE, as well as other LSMs which have no explicit dynamical representation of LAI. Finally, we also note that for a more complete assessment of the influence of LAI in LSMs, both the representation of vegetation through PFT maps and LAI variability should be analysed parallel to each other.

Acknowledgments.

All the authors except David Mocko are supported by the Australian Research Council Centre of Excellence for Climate System Science (CE110001028). This work was also supported by the NSW Environment Trust (RM08603). We thank CSIRO and the Bureau of Meteorology through the Centre for Australian Weather and Climate Research for their support in the use of the CABLE model. We thank the National Computational Infrastructure at the Australian National University, an initiative of the Australian Government, for access to supercomputer resources. We thank the NASA GSFC LIS team for support in coupling CABLE to LIS. The MODIS derived background soil albedo was provided by Peter R. J.

North from the Department of Geography, Swansea University, Swansea, United Kingdom. The modified MODIS LAI data was provided by Hua Yuan from from the Land-Atmosphere Interaction Research Group at Beijing Normal University. All of this assistance is gratefully acknowledged.

REFERENCES

Abramowitz, G. and H. Gupta, 2008: Toward a model space and model independence metric. *Geophys. Res. Lett.*, **35**, L05 705, doi:10.1029/2007GL032834.

Avila, F. B., A. J. Pitman, M. G. Donat, L. V. Alexander, and G. Abramowitz, 2012: Climate model simulated changes in temperature extremes due to land cover change. *J. Geophys. Res.*, **117**, D04 108, doi:10.1029/2011JD016382.

Barr, A. G., T. Black, E. Hogg, N. Kljun, K. Morgenstern, and Z. Nesic, 2004: Inter-annual variability in the leaf area index of a boreal aspen-hazelnut forest in relation to net ecosystem production. *Agricultural and Forest Meteorology*, **126**, 237 – 255, doi:10.1016/j.agrformet.2004.06.011.

Bonan, G. B., S. Levis, S. Sitch, M. Vertenstein, and K. W. Oleson, 2003: A dynamic global vegetation model for use with climate models: concepts and description of simulated vegetation dynamics. *Global Change Biology*, **9**, 1543–1566, doi:10.1046/j.1365-2486.2003.00681.x.

Bonan, G. B., D. Pollard, and S. L. Thompson, 1993: Influence of subgrid-scale heterogeneity in leaf area index, stomatal resistance, and soil moisture on grid-scale land-atmosphere interactions. *Journal of Climate*, **6**, 1882–1897, doi:10.1175/1520-0442(1993)006⟨1882:IOSSHI⟩2.0.CO;2.

Buermann, W., J. Dong, X. Zeng, R. B. Myneni, and R. E. Dickinson, 2001: Evaluation of the utility of satellite-based vegetation leaf area index data for climate simulations. *Journal of Climate*, **14**, 3536–3550, doi:10.1175/1520-0442(2001)014⟨3536:EOTUOS⟩2.0.CO;2.

Chase, T. N., R. A. Pielke, T. G. F. Kittel, R. Nemani, and S. W. Running, 1996: Sensitivity of a general circulation model to global changes in leaf area index. *J. Geophys. Res*, **101(D3)**, 73937408, doi:10.1029/95JD02417.

Cruz, F. T., A. J. Pitman, and Y.-P. Wang, 2010: Can the stomatal response to higher atmospheric carbon dioxide explain the unusual temperatures during the 2002 murray-darling basin drought? *J. Geophys. Res.*, **115 (D2)**, D02 101, doi:10.1029/2009JD012767.

Decker, M., A. J. Pitman, and J. P. Evans, 2012: Groundwater constraints on simulated transpiration variability over southeastern australian forests. *Journal of Hydrometeorology*, **in press**, doi:10.1175/JHM-D-12-058.1.

Dickinson, R. E., M. Shaikh, R. Bryant, and L. Graumlich, 1998: Interactive canopies for a climate model. *Journal of Climate*, **11**, 2823–2836.

Dirmeyer, P. A., X. Gao, M. Zhao, Z. Guo, T. Oki, and N. Hanasaki, 2006: Supplement to GSWP-2: Details of the forcing data. *Bulletin of the American Meteorological Society*, **87**, S10–S16, doi:10.1175/BAMS-87-10-Dirmeyer.

Dorman, J. L. and P. J. Sellers, 1989: A global climatology of albedo, roughness length and stomatal resistance for atmospheric general circulation models as represented by the simple biosphere model (SiB). *Journal of Applied Meteorology*, **28**, 833–855, doi:10.1175/1520-0450(1989)028⟨0833:AGCOAR⟩2.0.CO;2.

Duursma, R., et al., 2009: Contributions of climate, leaf area index and leaf physiology to variation in gross primary production of six coniferous forests across Europe: a model-based analysis. *Tree Physiology*, **29 (5)**, 621–639, doi:10.1093/treephys/tpp010.

Exbrayat, J.-F., A. J. J. Pitman, G. Abramowitz, and Y.-P. Wang, 2012: Sensitivity of net ecosystem exchange and heterotrophic respiration to parameterization uncertainty. *J. Geophys. Res.*, doi:10.1029/2012JD018122,inpress.

Guillevic, P., R. D. Koster, M. J. Suarez, L. Bounoua, G. J. Collatz, S. O. Los, and S. P. P. Mahanama, 2002: Influence of the interannual variability of vegetation on the surface energy balance—a global sensitivity study. *Journal of Hydrometeorology*, **3**, 617–629, doi: 10.1175/1525-7541(2002)003⟨0617:IOTIVO⟩2.0.CO;2.

Haverd, V., et al., 2013: Multiple observation types reduce uncertainty in Australia's terrestrial carbon and water cycles. *Biogeosciences*, **10**, 2011–2040, doi:10.5194/bg-10-2011-2013.

Houldcroft, C. J., W. M. F. Grey, M. Barnsley, C. M. Taylor, S. O. Los, and P. R. J. North, 2009: New vegetation albedo parameters and global fields of soil background albedo derived from MODIS for use in a climate model. *Journal of Hydrometeorology*, **10**, 183–198, doi:10.1175/2008JHM1021.1.

Jones, D., W. Wang, and R. Fawcett, 2009: High-quality spatial climate data-sets for Australia. *Australian Meteorology Magazine*, **58**, 233–248.

Jung, M., M. Reichstein, and A. Bondeau, 2009: Towards global empirical upscaling of fluxnet eddy covariance observations: validation of a model tree ensemble approach using a biosphere model. *Biogeosciences*, **6 (10)**, 2001–2013, doi:10.5194/bg-6-2001-2009.

Keeling, C. D., S. C. Piper, R. B. Bacastow, M. Wahlen, T. P. Whorf, M. Heimann, and H. A. Meijer, 2005: Atmospheric CO_2 and $^{13}CO_2$ exchange with the terrestrial biosphere and oceans from 1978 to 2000: observations and carbon cycle implications, pages 83-113, in "A history of atmospheric CO_2 and its effects on plants, animals, and ecosystems", editors, Ehleringer, J.R., T. E. Cerling, M. D. Dearing, Springer Verlag, New York.

Keith, H., E. van Gorsel, K. Jacobsen, and H. Cleugh, 2012: Dynamics of carbon exchange in a eucalyptus forest in response to interacting disturbance factors. *Agricultural and Forest Meteorology*, **153**, 67 – 81, doi:10.1016/j.agrformet.2011.07.019.

Kowalczyk, E. A., Y. P. Wang, R. M. Law, H. L. Davies, J. L. McGregor, and G. Abramowitz, 2006: The CSIRO Atmosphere Biosphere Land Exchange model for use in climate models and as an offline model. Commonwealth Scientific and Industrial Research Organisation Marine and Atmospheric Research Paper 013, November 2006, 37 pages, online accessed at: `www.cmar.csiro.au/e-print/open/kowalczykea_2006a.pdf`. URL `http://www.cmar.csiro.au/e-print/open/kowalczykea_2006a.pdf`, URL `http://www.cmar.csiro.au/e-print/open/kowalczykea_2006a.pdf`.

Kumar, S., et al., 2006: Land information system: An interoperable framework for high resolution land surface modeling. *Environmental Modelling and Software*, **21**, 1402 – 1415, doi:10.1016/j.envsoft.2005.07.004.

Kumar, S. V., C. D. Peters-Lidard, J. L. Eastman, and W.-K. Tao, 2008: An integrated high-resolution hydrometeorological modeling testbed using lis and wrf. *Environmental Modelling and Software*, **23**, 169 – 181, doi:10.1016/j.envsoft.2007.05.012.

Li, L., Y. P. Wang, Q. Yu, B. Pak, D. Eamus, J. Yan, E. van Gorsel, and I. Baker, 2012: Improving the responses of the australian community land surface model (cable) to seasonal drought. *J. Geophys. Res.*, doi:10.1029/2012JG002038.inpress.

Liu, Q., L. Gu, R. E. Dickinson, Y. Tian, L. Zhou, and W. M. Post, 2008: Assimilation of satellite reflectance data into a dynamical leaf model to infer seasonally varying leaf areas for climate and carbon models. *Journal of Geophysical Research: Atmospheres*, **113 (D19)**, doi:10.1029/2007JD009645.

Lu, X., Y.-P. Wang, T. Ziehn, and Y. Dai, 2013: An efficient method for global parameter sensitivity analysis and its applications to the Australian community land surface model (CABLE). *Agricultural and Forest Meteorology*, **in press**, doi:http://dx.doi.org/10.1016/j.agrformet.2013.04.003.

Mao, J., S. J. Phipps, A. J. Pitman, Y. P. Wang, G. Abramowitz, and B. Pak, 2011: The

570 CSIRO Mk3L climate system model v1.0 coupled to the CABLE land surface scheme
571 v1.4b: evaluation of the control climatology. *Geoscientific Model Development*, **4 (4)**,
572 1115–1131, doi:10.5194/gmd-4-1115-2011.

573 McColl, K. A., R. C. Pipunic, D. Ryu, and J. P. Walker, 2011: Validation of the MODIS
574 LAI product in the Murrumbidgee catchment, Australia, 19th International Congress on
575 Modelling and Simulation, Perth, Australia, 12-16 December 2011.

576 Parton, W., A. Haxeltine, P. Thornton, R. Anne, and M. Hartman, 1996: Ecosystem sensi-
577 tivity to land-surface models and leaf area index. *Global and Planetary Change*, **13**, 89 –
578 98, doi:10.1016/0921-8181(95)00040-2.

579 Piao, S., P. Friedlingstein, P. Ciais, N. Viovy, and J. Demarty, 2007: Growing season exten-
580 sion and its impact on terrestrial carbon cycle in the northern hemisphere over the past 2
581 decades. *Global Biogeochemical Cycles*, **21**, doi:10.1029/2006GB002888.

582 Pielke, R. A., T. J. Lee, J. H. Copeland, J. L. Eastman, C. L. Ziegler, and C. A. Finley,
583 1997: Use of usgs-provided data to improve weather and climate simulations. *Ecological*
584 *Applications*, **7**, 3–21, doi:10.1890/1051-0761(1997)007{$[$}0003:UOUPDT{$]$}2.0.CO;
585 2.

586 Pitman, A. J., 2003: The evolution of, and revolution in, land surface schemes designed for
587 climate models. *International Journal of Climatology*, **23**, 479–510, doi:10.1002/joc.893.

588 Pitman, A. J., F. B. Avila, G. Abramowitz, Y. P. Wang, S. J. Phipps, and N. de Noblet-
589 Ducoudré, 2011: Importance of background climate in determining impact of land-cover
590 change on regional climate. *Nature Climate Change*, **9 (1)**, 472–475.

591 Pitman, A. J., M. Zhao, and C. E. Desborough, 1999: Investigating the sensitivity of a land
592 surface scheme's simulation of soil wetness and evaporation to spatial and temporal leaf
593 area index variability within the global soil wetness project. *Journal of the Meteorological*
594 *Society of Japan. Ser. II*, **77**, 281–290.

595 Puma, M. J., R. D. Koster, and B. I. Cook, 2013: Phenological versus meteorological controls
596 on land-atmosphere water and carbon fluxes. *Journal of Geophysical Research: Biogeo-*
597 *sciences*, doi:10.1029/2012JG002088.

598 Raupach, M. R., 1994: Simplified expressions for vegetation roughness length and zero-plane
599 displacement as functions of canopy height and area index. *Boundary-Layer Meteorology*,
600 **71**, 211–216.

601 Rienecker, M. M., et al., 2011: MERRA: NASA's Modern-Era Retrospective Analy-
602 sis for Research and Applications. *Journal of Climate*, **24**, 3624–3648, doi:10.1175/
603 JCLI-D-11-00015.1.

604 Risbey, J. S., M. J. Pook, P. C. McIntosh, M. C. Wheeler, and H. H. Hendon, 2009: On
605 the remote drivers of rainfall variability in australia. *Monthly Weather Review*, **137**, 3233–
606 3253, doi:10.1175/2009MWR2861.1.

607 Rodell, M., et al., 2004: The global land data assimilation system. *Bulletin of the American*
608 *Meteorological Society*, **85**, 381–394, doi:10.1175/BAMS-85-3-381.

609 Saigusa, N., et al., 2008: Temporal and spatial variations in the seasonal patterns of co2 flux
610 in boreal, temperate, and tropical forests in East Asia. *Agricultural and Forest Meteorology*,
611 **148**, 700 – 713, doi:10.1016/j.agrformet.2007.12.006.

612 van den Hurk, B. J. J. M., P. Viterbo, and S. O. Los, 2003: Impact of leaf area index sea-
613 sonality on the annual land surface evaporation in a global circulation model. *J. Geophys.*
614 *Res.*, **108**, 4191, doi:10.1029/2002JD002846.

615 Verstraete, M. and R. Dickinson, 1986: Modeling surface processes in atmospheric general
616 circulation models. *Annales Geophysicae*, **4**, 357–364.

617 Wang, Y. P., E. Kowalczyk, R. Leuning, G. Abramowitz, M. R. Raupach, B. Pak, E. van

Gorsel, and A. Luhar, 2011: Diagnosing errors in a land surface model (CABLE) in the time and frequency domains. *J. Geophys. Res.*, **116**, G01 034, doi:10.1029/2010JG001385.

Wang, Y.-P. and R. Leuning, 1998: A two-leaf model for canopy conductance, photosynthesis and partitioning of available energy i:: Model description and comparison with a multi-layered model. *Agricultural and Forest Meteorology*, **91**, 89 – 111, doi:10.1016/S0168-1923(98)00061-6.

Wang, Y. P., X. J. Lu, I. J. Wright, Y. J. Dai, P. J. Rayner, and P. B. Reich, 2012: Correlations among leaf traits provide a significant constraint on the estimate of global gross primary production. *Geophys. Res. Lett.*, **39 (19)**, L19 405, doi:10.1029/2012GL053461.

White, M. A. and R. R. Nemani, 2003: Canopy duration has little influence on annual carbon storage in the deciduous broad leaf forest. *Global Change Biology*, **9**, 967–972, doi:10.1046/j.1365-2486.2003.00585.x.

Yuan, H., Y. Dai, Z. Xiao, D. Ji, and W. Shangguan, 2011: Reprocessing the MODIS leaf area index products for land surface and climate modelling. *Remote Sensing of Environment*, **115**, 1171 – 1187, doi:10.1016/j.rse.2011.01.001.

Zhang, H., B. Pak, Y. P. Wang, X. Zhou, Y. Zhang, and L. Zhang, 2013: Evaluating surface water cycle simulated by the Australian Community Land Surface Model (CABLE) across different spatial and temporal domains. *Journal of Hydrometeorology*, **in press**, doi:10.1175/JHM-D-12-0123.1.

Zhang, H., L. Zhang, and B. Pak, 2011a: Comparing surface energy, water and carbon cycle in dry and wet regions simulated by a land-surface model. *Theoretical and Applied Climatology*, **104**, 511–527, doi:10.1007/s00704-010-0364-x.

Zhang, Q., Y. P. Wang, A. J. Pitman, and Y. J. Dai, 2011b: Limitations of nitrogen and phosphorous on the terrestrial carbon uptake in the 20th century. *Geophys. Res. Lett.*, **38 (22)**, L22 701, doi:10.1029/2011GL049244.

List of Tables

Table 1: Zero-lag cross-correlations between differences in leaf area index (LAI) and differences in: vegetation transpiration (EV), soil evaporation (ES), sensible heat (Qh), latent heat (Qle), autotrophic respiration (AR), heterotrophic respiration (HR), and gross primary production (GPP) for the major PFT shown in Figure 2.

PFTs	EV	ES	Qh	Qle	AR	HR	GPP
Open shrublands	0.94	-0.90	-0.63	0.39	0.91	-0.76	0.99
Croplands	0.88	-0.90	0.20	-0.29	0.87	-0.56	0.95
Woody savannas	0.97	-0.88	0.31	-0.64	0.95	-0.40	0.99
Evergreen broadleaf trees	0.80	-0.88	0.63	-0.76	0.79	0.46	0.87
Savannas	0.93	-0.88	0.46	-0.65	0.91	-0.48	0.97
Grasslands	0.90	-0.80	-0.29	0.01	0.85	-0.66	0.98

List of Figures

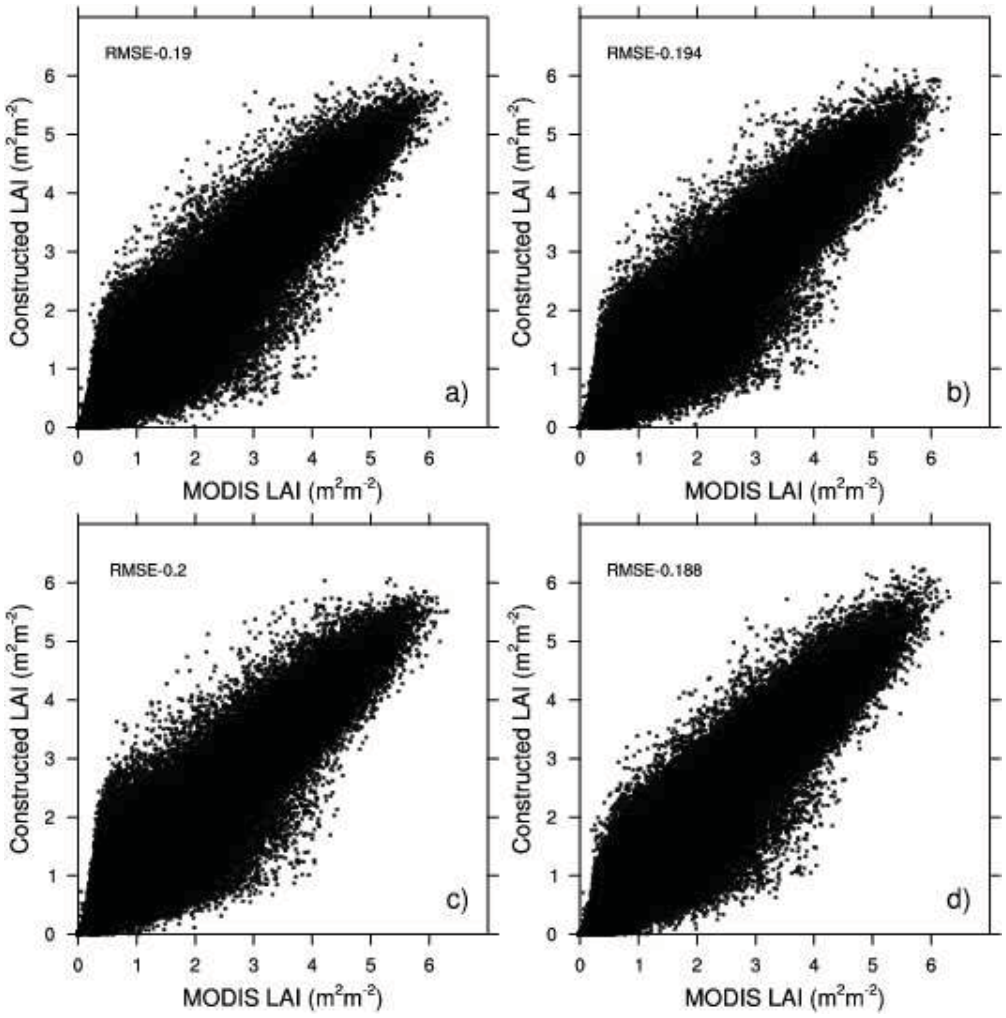

Figure 1: Scatter plot of the ensemble mean of the constructed LAI (m^2 m^{-2}) versus the MODIS LAI (m^2 m^{-2}) for each grid cell for the period 2000-2008 obtained using (a) precipitation, (b) minimum temperature, (c) maximum temperature, and (d) precipitation, and minimum and maximum temperature.

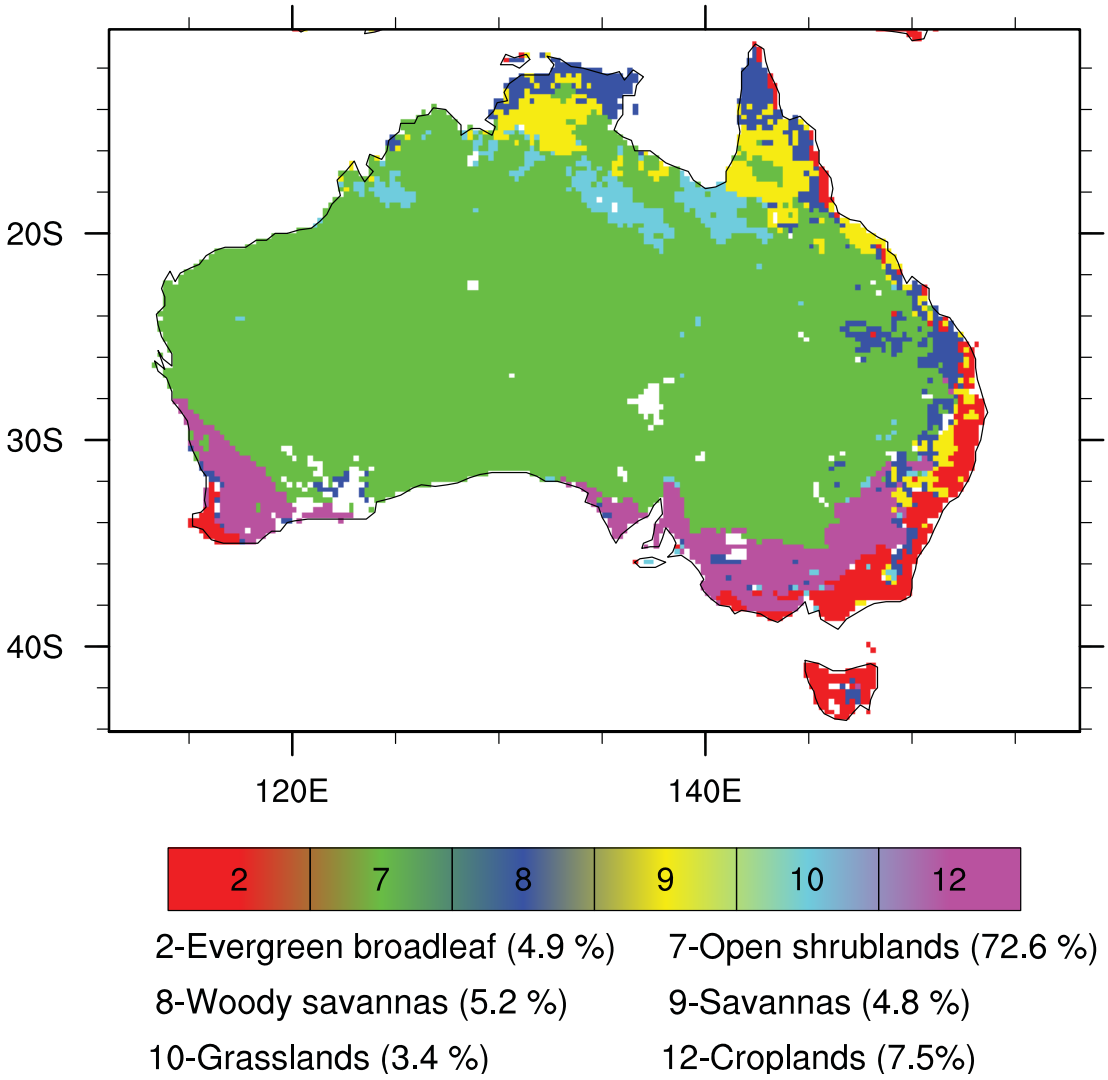

Figure 2: Dominant plant functional types (PFTs), defined as greater than 1% of land points (masked inland regions in white are PFTs less than 1% of land points).

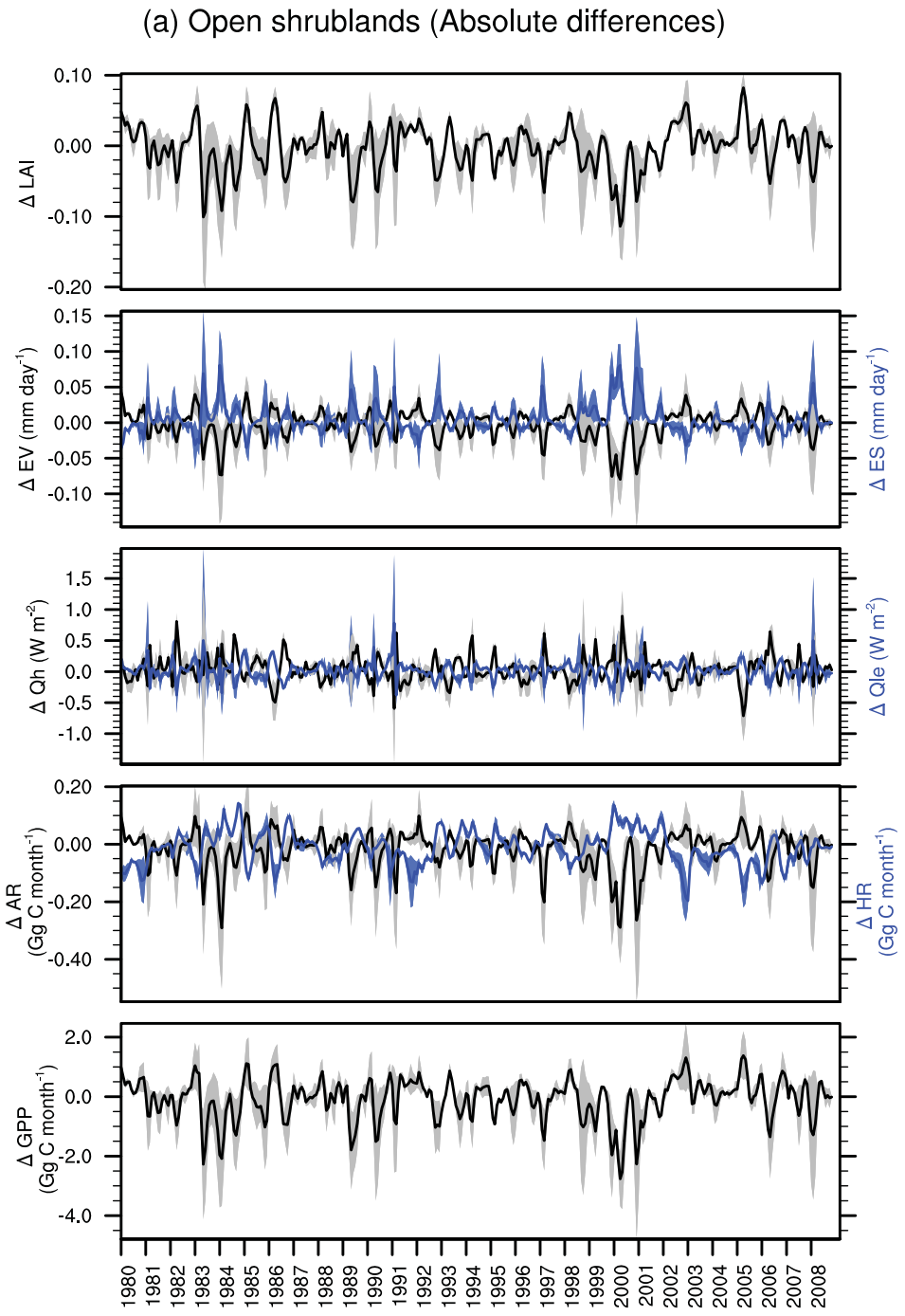

Figure 3: Time series of (a) monthly mean absolute differences, and (b) percentage differences (next page), in LAI, vegetation transpiration (EV), soil evaporation (ES), sensible heat (Qh), latent heat (Qle), autotrophic respiration (AR), heterotrophic respiration (HR), and gross primary production (GPP) between the control simulation and the ensemble mean for open shrublands (72.6 % of land points). The shaded region represents one standard deviation.

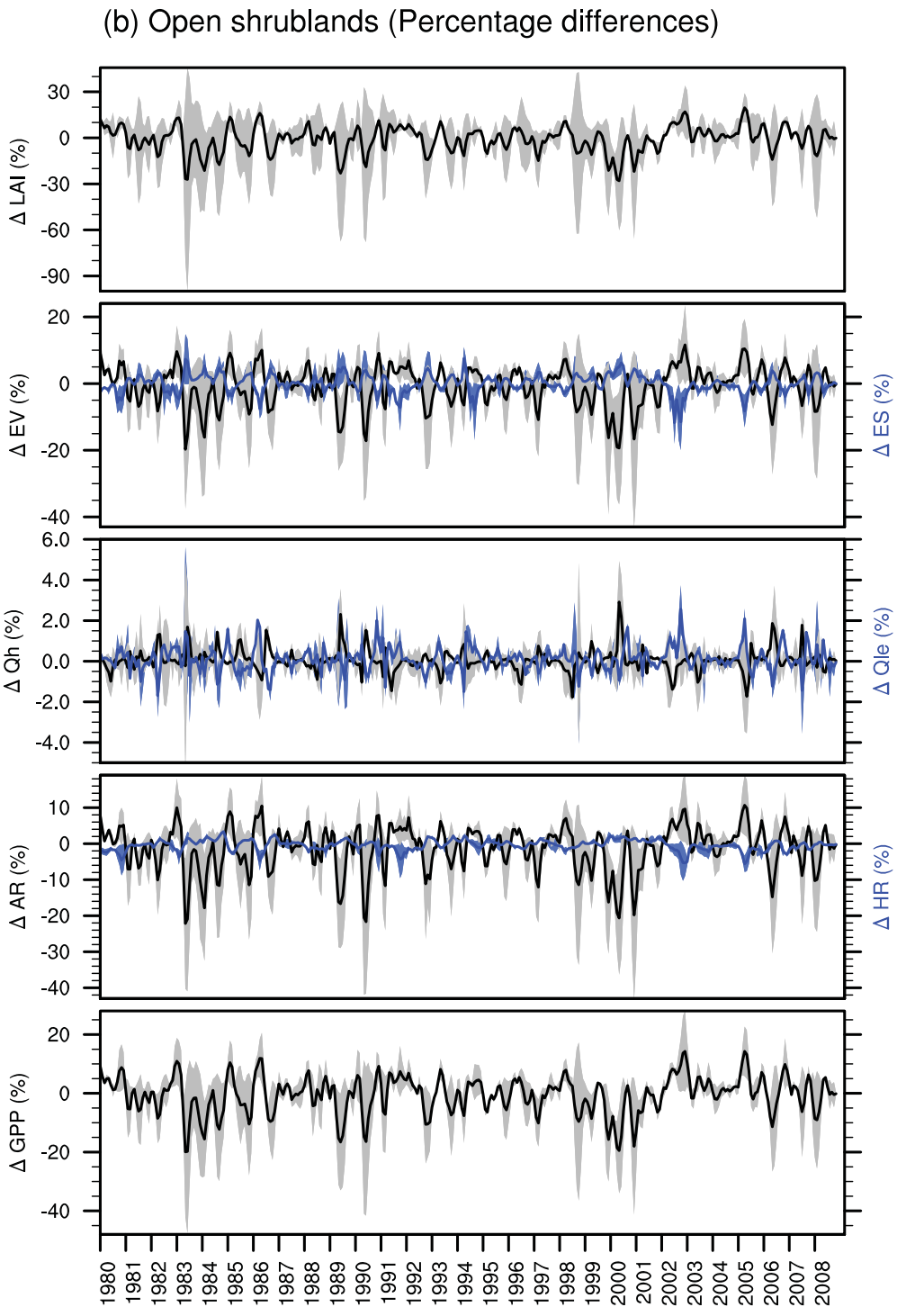

Figure 3: Continued

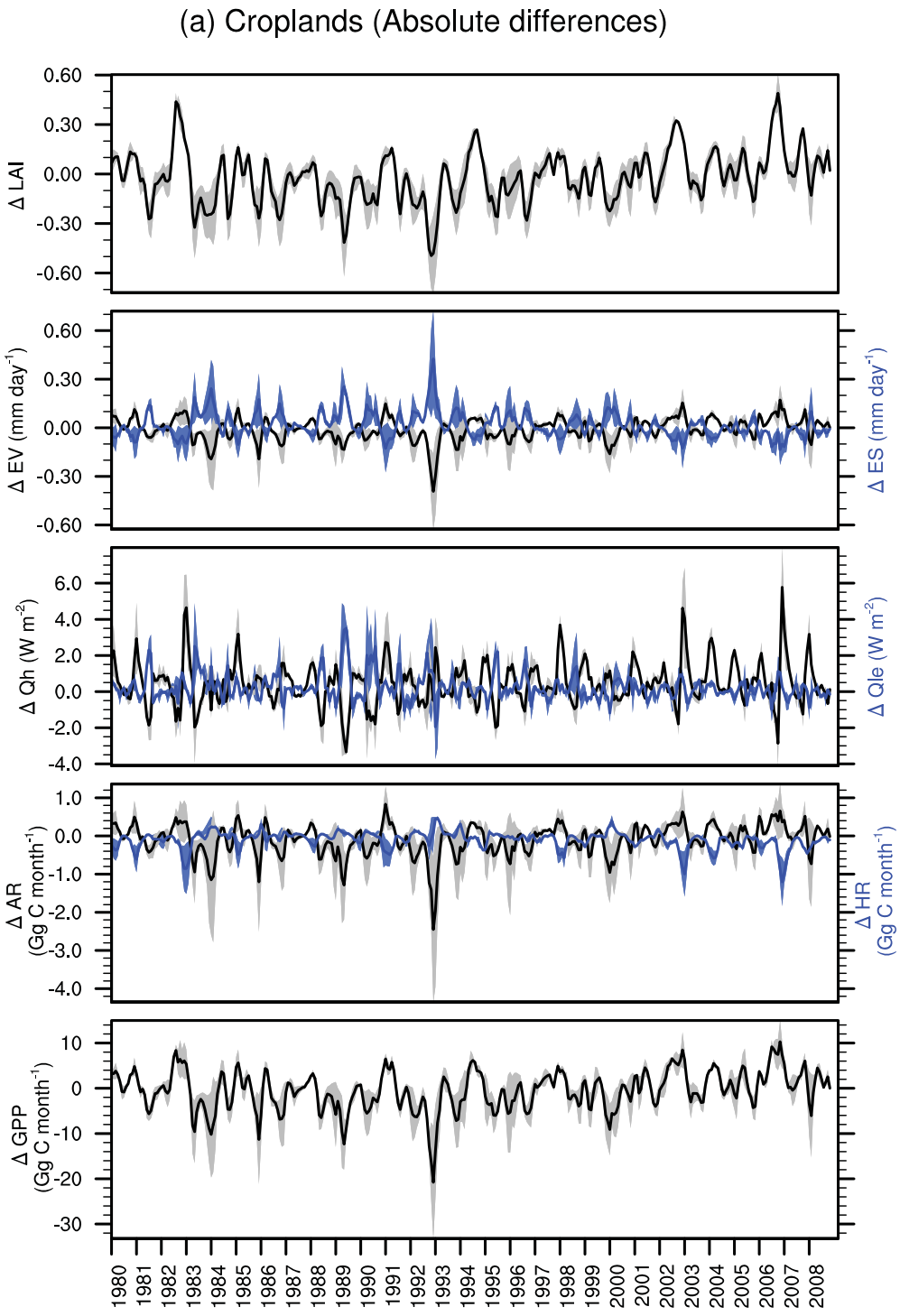

Figure 4: Same as in Figure 3 but for for croplands (7.5 % of land points).

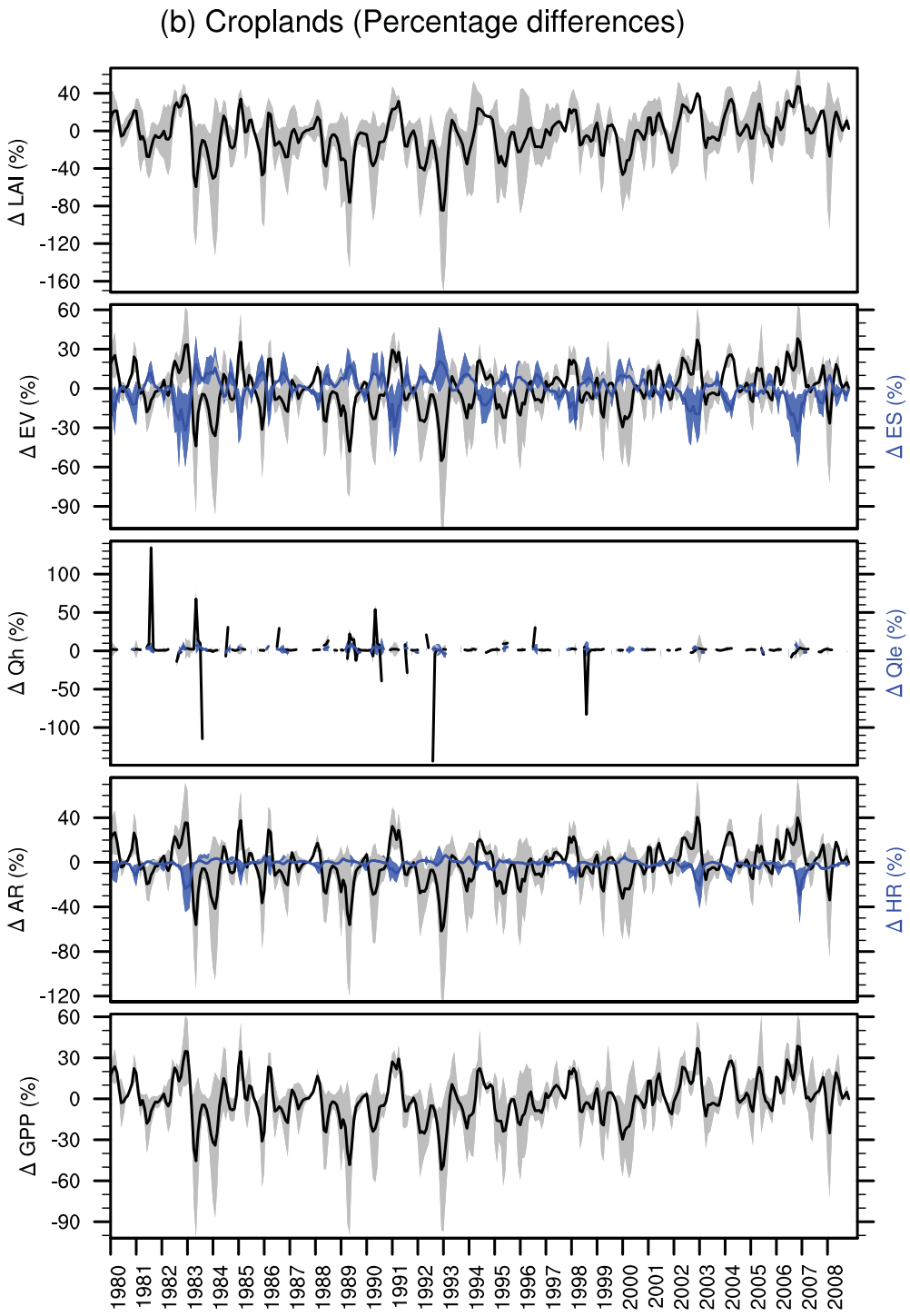

Figure 4: Continued

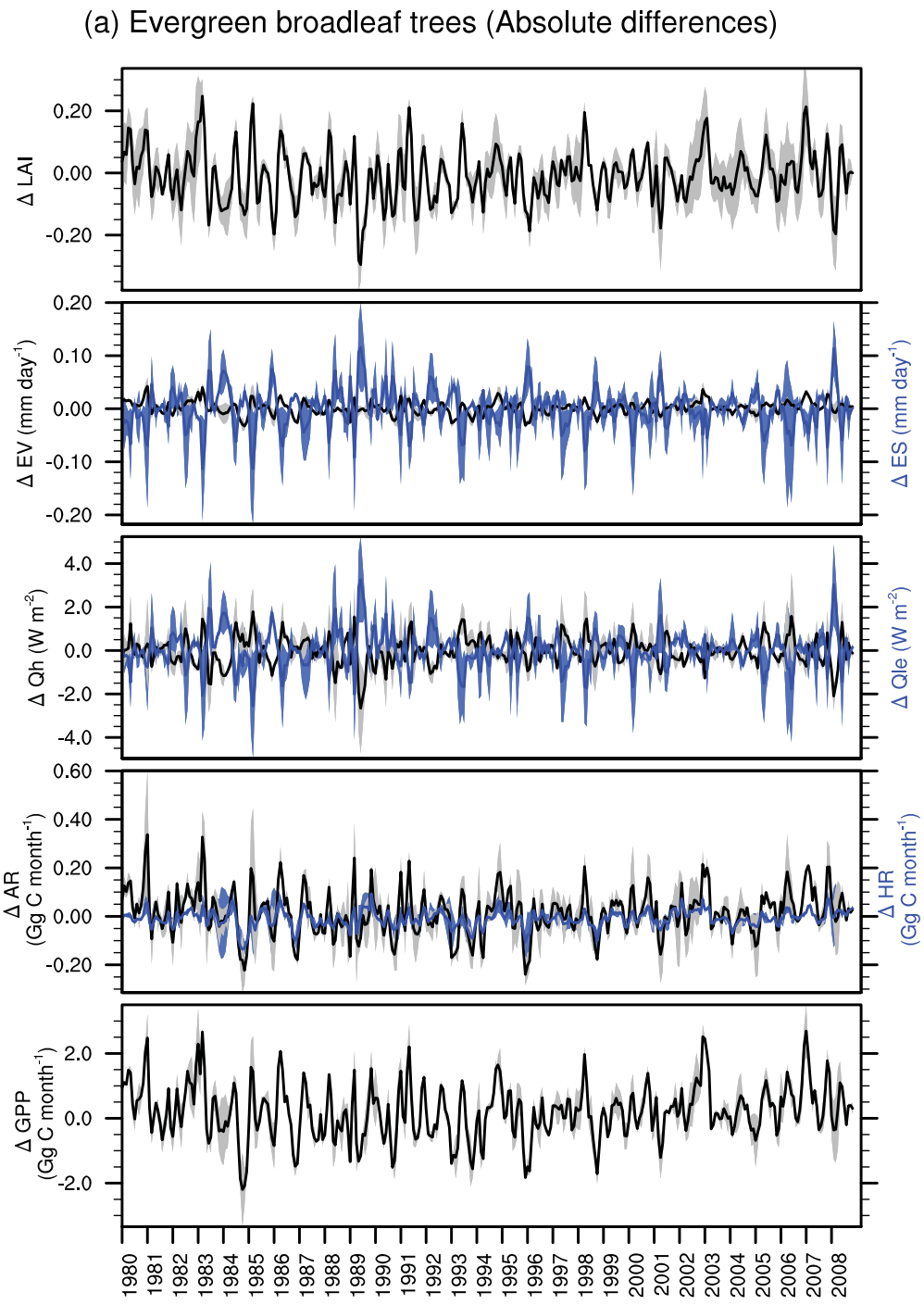

Figure 5: Same as in Figure 3 but for for evergreen broadleaf trees (4.9 % of land points).

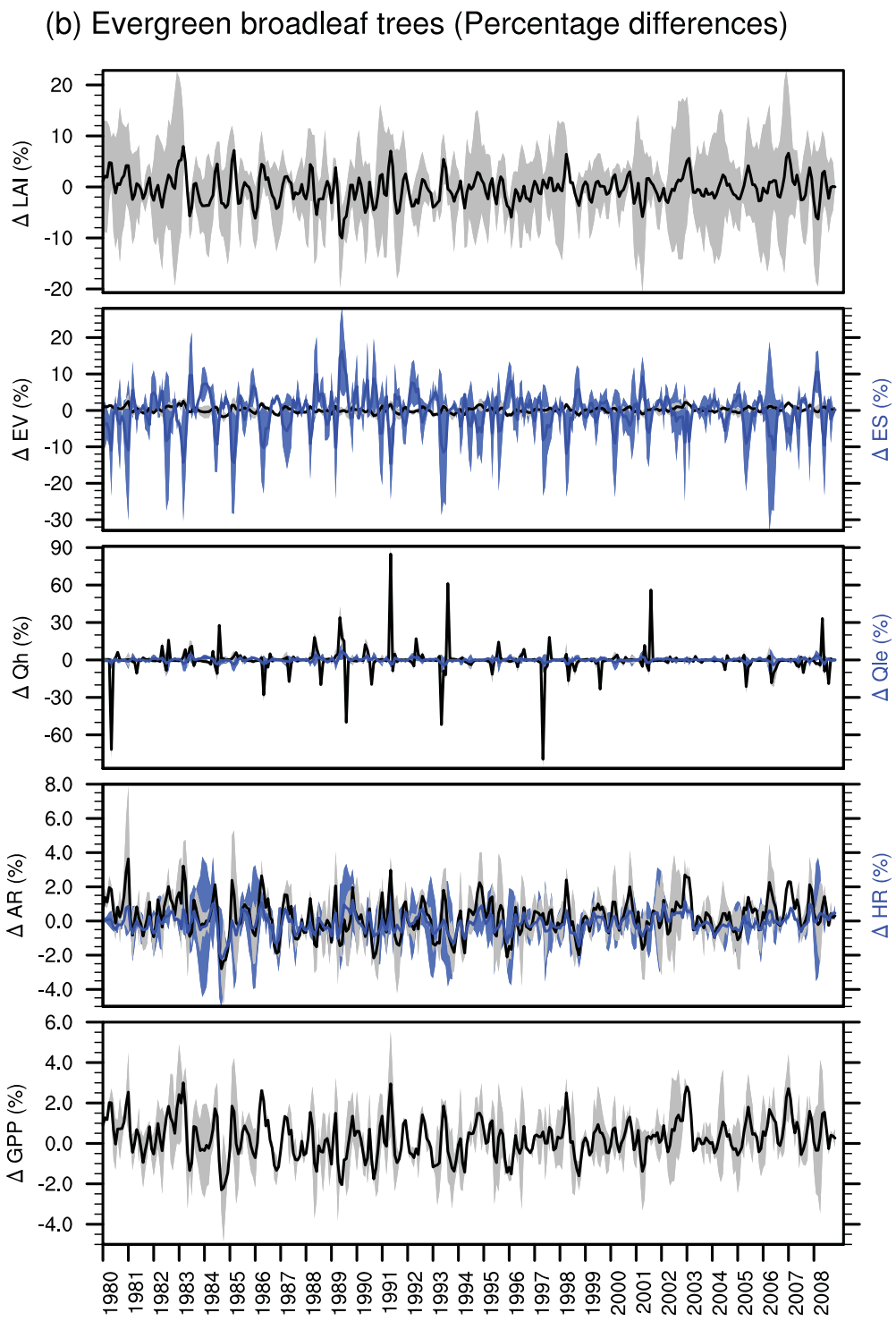

Figure 5: Continued

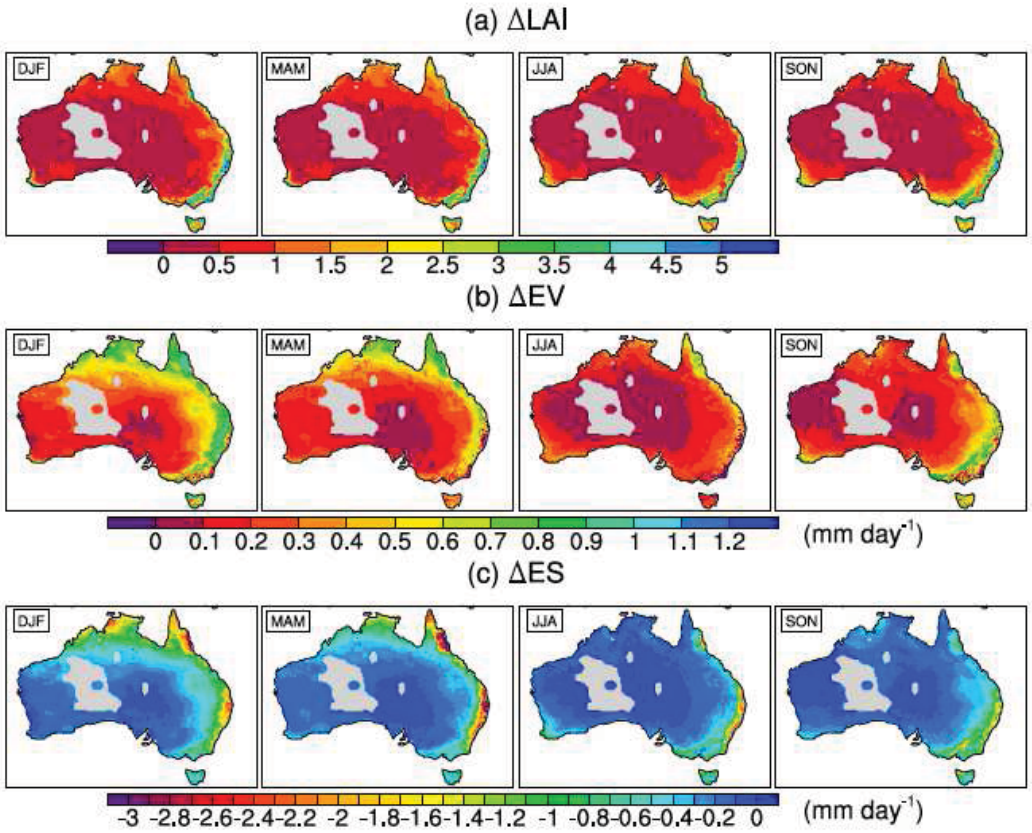

Figure 6: Differences in (a) LAI, (b) vegetation evaporation (EV) (mm day^{-1}), and (c) soil evaporation (ES) (mm day^{-1}) between the experiment with +50% and -50% of the control LAI (the masked inland areas are regions where the gridded precipitation data used to generate the LAI ensemble was missing, and hence these points were excluded from all analysis for consistency).

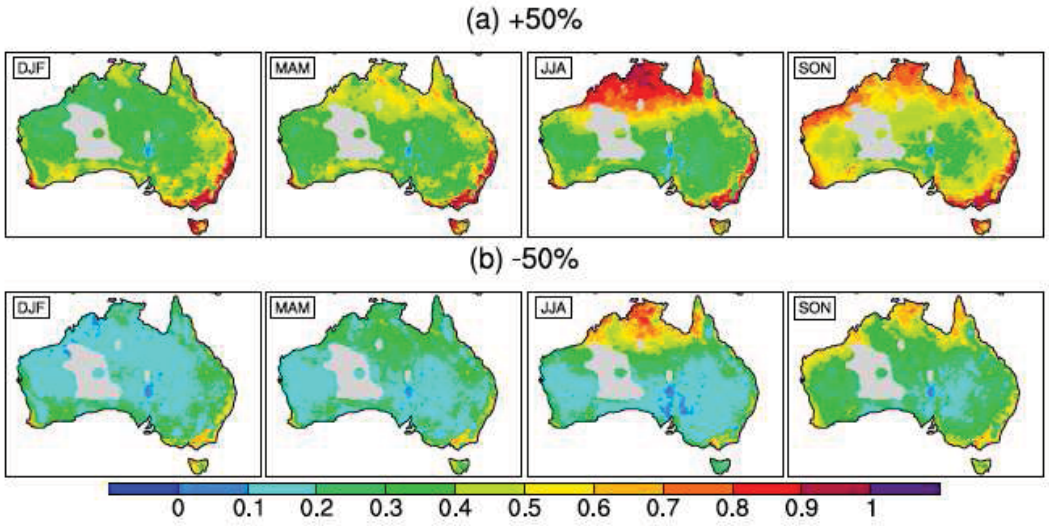

Figure 7: Ratio of vegetation evaporation to total evapotranspiration (i.e., EV/(ES+EV)) for the experiments with (a) +50% of the control LAI, and (b) -50 % of the control LAI.

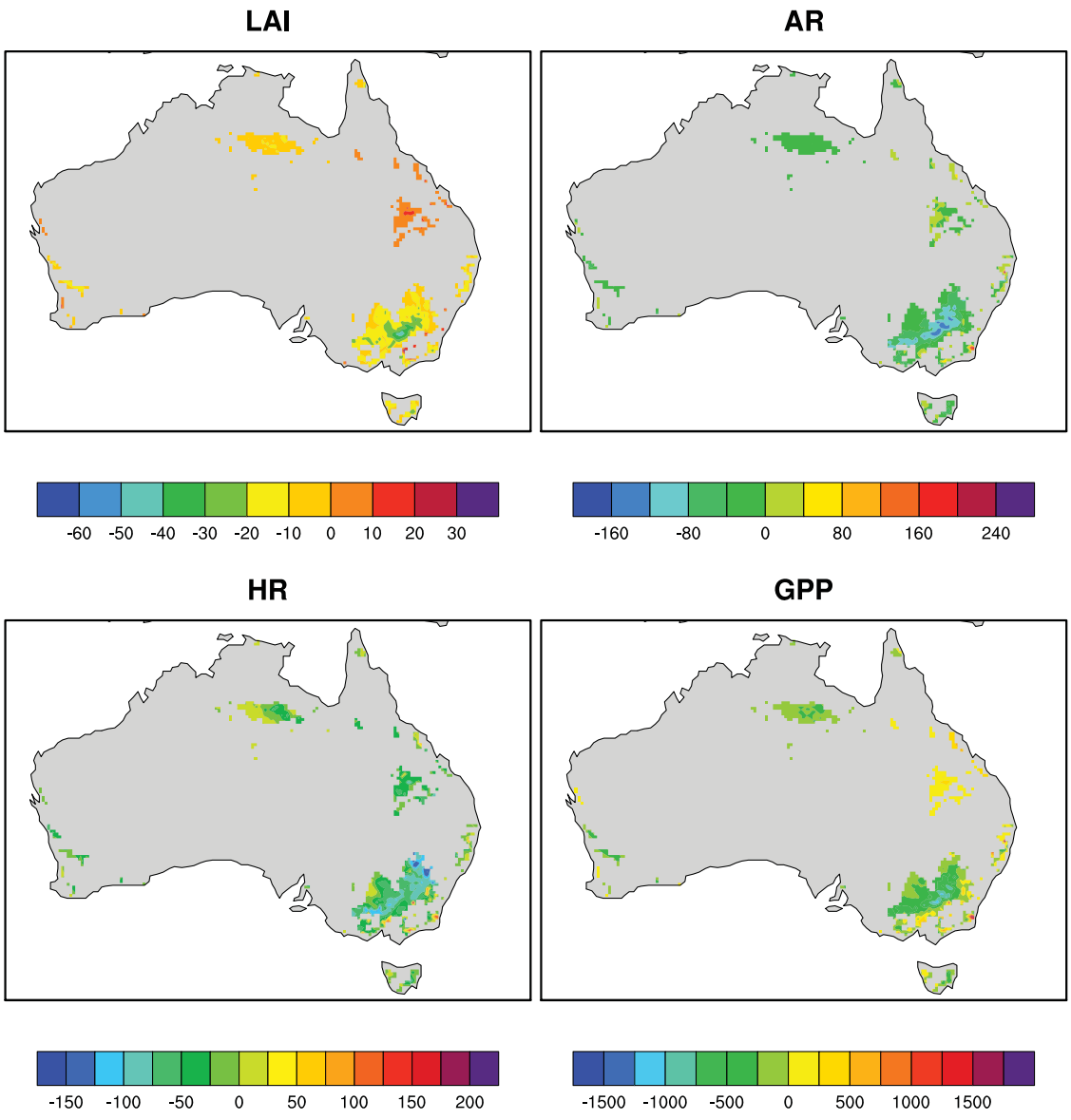

Figure 8: Gridded cumulative difference in monthly mean LAI and carbon fluxes (Gg month^{-1}) between the control simulation and the ensemble mean (cumulative changes in LAI < 5 have been masked out to highlight the largest changes).

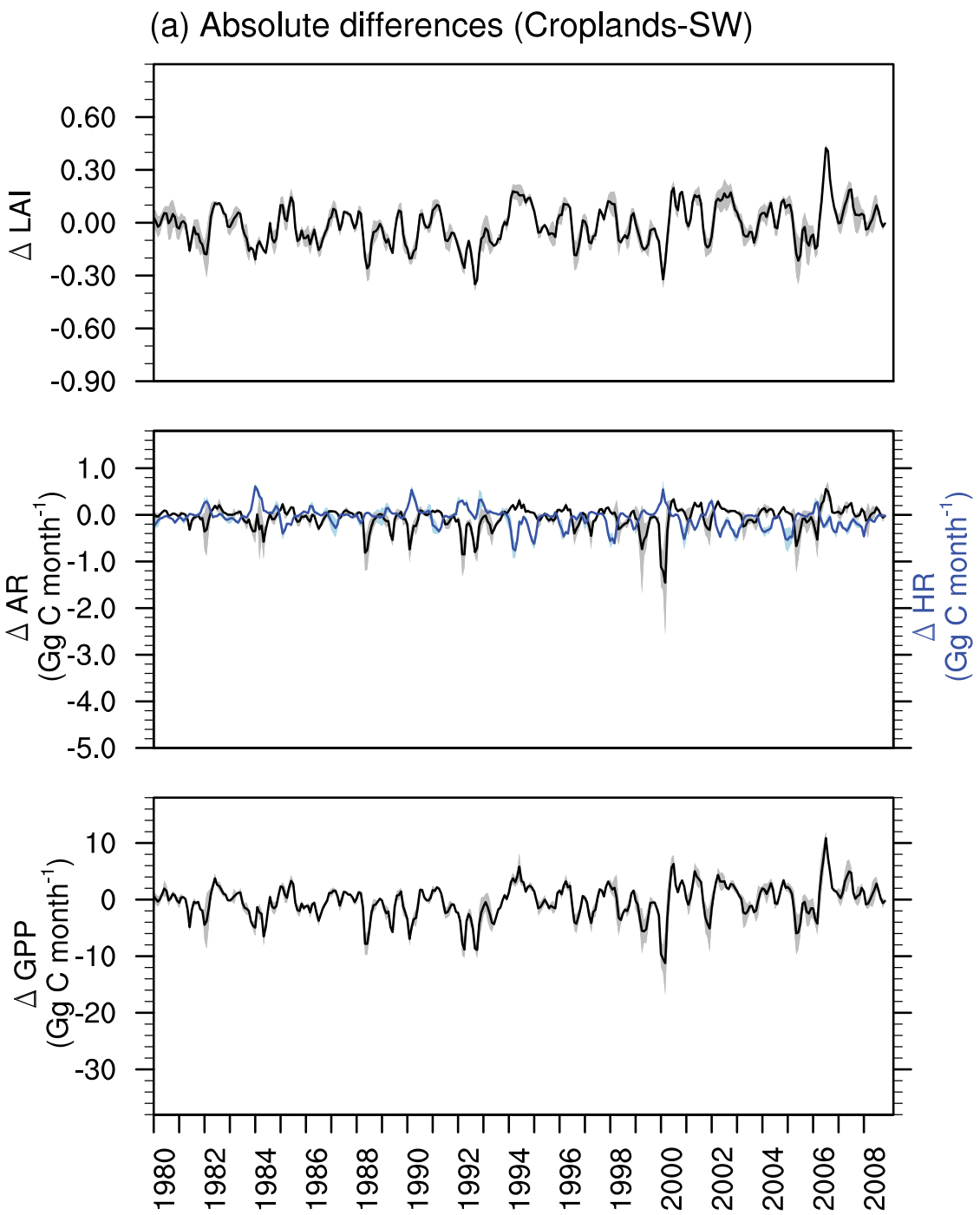

Figure 9: Time series of monthly mean absolute differences in LAI, autotrophic respiration (AR), heterotrophic respiration (HR), and gross primary production (GPP) between the control simulation and the ensemble mean for (a) southwestern (SW) croplands, and (b) southeastern (SE) croplands (next page).

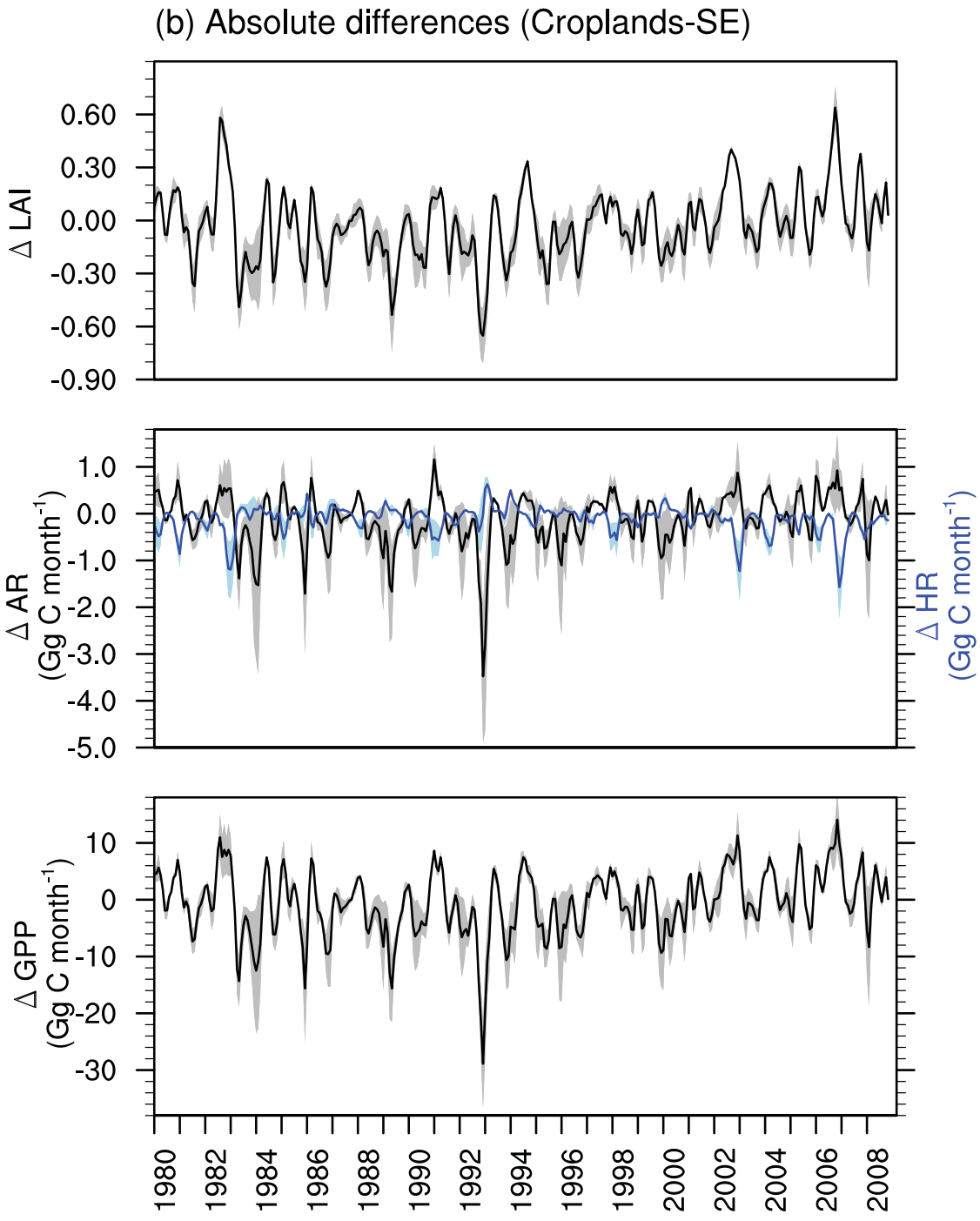

Figure 9: Continued